PHYSICAL REVIEW B **78**, 121302(R) (2008)

Diffusionlike electric-field migration in the channel of organic field-effect transistors

Takaaki Manaka,[1,*] Fei Liu,[2] Martin Weis,[1] and Mitsumasa Iwamoto[1,†]
[1]*Department of Physical Electronics, Tokyo Institute of Technology, 2-12-1 O-okayama, Meguro-ku, Tokyo 152-8552, Japan*
[2]*Center for Advanced Study, Tsinghua University, Beijing, 100084, China*
(Received 27 July 2008; revised manuscript received 28 August 2008; published 17 September 2008)

Time-resolved microscopic optical second-harmonic generation (TRM-SHG) technique provides a different approach to study the dynamics of carriers in organic field-effect transistor (OFET). Different from many common methods, the TRM SHG directly probes the transient electric-field distribution in the channel of the OFET in high temporal and spatial resolutions. In this work we used this technique to quantitatively study migration of the peak of the electric field. We found that under a broad range of experimental conditions, the migration of the peak of the electric field follows a diffusionlike behavior; namely, the square of the peak position of $\bar{x}$ is proportional to time t. Based on a two-dimensional computational simulation and general carrier transport mechanism, we proposed that this behavior arises from a simple relation, $\mu \simeq \gamma \bar{x}^2/(t|V_{gs}|)$, where μ is the carrier mobility, γ is constant about 0.5, and V_{gs} is the gate voltage with respect to the source voltage. The experimental and simulation data well supported this relationship.

DOI: 10.1103/PhysRevB.78.121302 PACS number(s): 78.47.jc, 42.65.−k, 73.50.−h, 73.61.Ph

Understanding carrier motion in materials is one of the most fundamental subjects in physics, material science, electronics and electric engineering.[1,2] In the past 50 years, many experimental techniques were developed for this purpose including Haynes-Shockley experiment on the transit times of injected carriers,[3] time-of-flight (TOF) experiment for the determination of carrier mobility,[4] pressure-wave propagation experiment for probing electric-field distribution in insulators,[5] organic monolayer experiment for probing orientational dipolar changes,[6] and etc. According to these results, theoretical studies of carrier transport have been conducted systematically based on a one-dimensional (1D) carrier analysis.[7–9] Most of these techniques are based on the measurement of current. For instance, the most widely used technique of TOF explores the Maxwell's displacement current generated by 1D dynamic carrier motion between two parallel electrodes.[4] Although current could be readily measured by electric instruments, a task of extracting useful physical information from the current is nontrivial because no simple relationship exists between the current and the carrier motion.[7]

Recently, we developed a time-resolved microscopic optical second-harmonic generation (TRM-SHG) technique[10] for visualizing the carrier motion in organic field-effect transistor (OFET); see Fig. 1(a). Different from the techniques mentioned above, this approach directly probes the transient electric-field distribution in the channel of the OFET by a two-photon process. Using a high-sensitivity charge-coupled device (CCD) as a detector, this approach has achieved considerably high temporal and spatial resolutions. In this Rapid Communication, we quantitatively studied the migration of the electric field in the channel of the OFET in terms of the TRM-SHG experiment and theory. We found that this migration follows a diffusionlike behavior; namely, the square root of the peak position of the electric field is proportional to time. Based on a two-dimensional (2D) computational simulation and a general physical analysis, we argued that the diffusionlike migration of the electric field along the channel of the OFET could arise from a self-consistent interaction between the carriers and electric field. A simple formula that connects the carrier mobility, the peak position of the electric field, time, and the gate-source voltage was proposed. Both the experimental and simulation results well supported this relationship.

Samples used in the experiments were top-contact pentacene OFETs [see Fig. 1(a)]. Heavily doped Si wafers were used as the base substrates, and they were covered with a 500-nm-thick silicon dioxide (SiO_2) insulating layer. Before the pentacene deposition, 100 nm thick of poly(methyl methacrylate) layer was spin coated, and the pentacene layer, approximately 100 nm thick, was deposited. After the deposition of pentacene, top-Au electrodes (the source and drain electrodes) with a thickness of 100 nm were deposited on the pentacene surface. The designed channel length and width were 30 μm and 3 mm, respectively. Pentacene FETs were operated with the application of pulse voltages using a func-

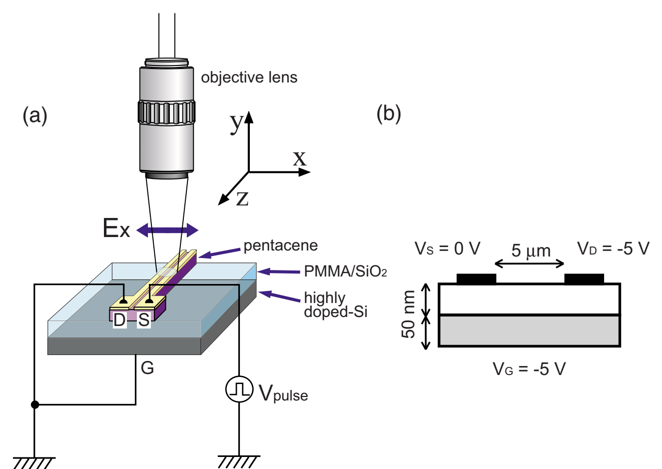

FIG. 1. (Color online) Device configuration of the TRM-SHG measurement. (a) Schematic diagram of the OFET device and electrical connection. Using microscopic objectives, fundamental light is focused on the device. (b) Schematic diagram of the cross section (x-y plane) of the top-contact OFET structure and the parameters for simulation. The thicknesses of the pentacene film (empty region) and insulator (gray region) are the same.

 ©2008 The American Physical Society

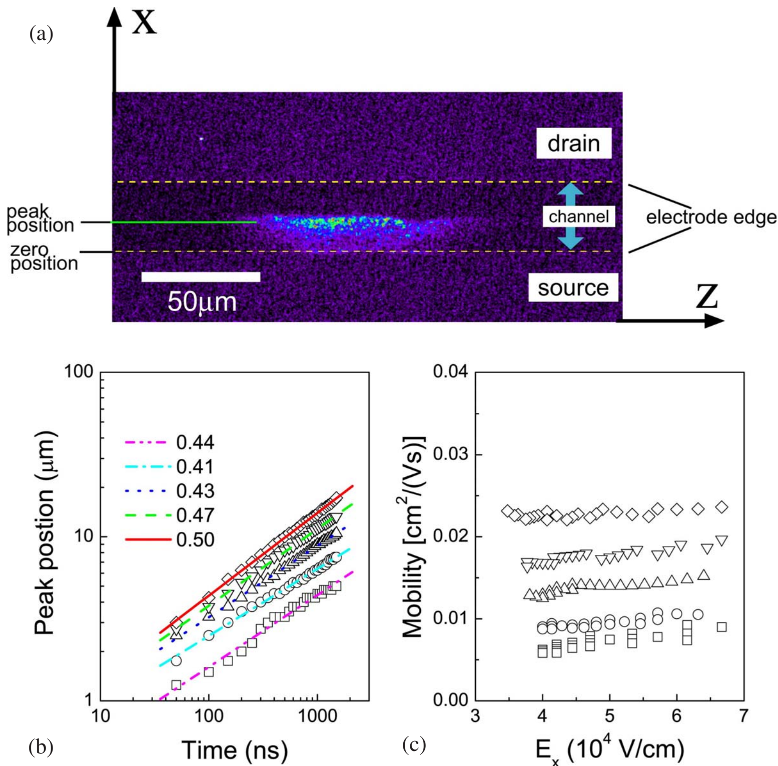

FIG. 2. (Color online) (a) Typical experimental result of the TRM-SHG imaging at a delay time of 100 ns under $V_{gs}=-100$ V. (b) The peak position of the SHG intensity vs time. The applied V_{gs} are −20 V (square), −30 V (circles), −40 V (upper triangles), −50 V (lower triangles), and −60 V (diamonds), respectively. The lines are the corresponding fittings and their slopes were listed. (c) The mobility evaluated by Eq. (3) with $\gamma=0.7$ vs the electric field $E_x(\bar{x})$ evaluated by $-V_{gs}/\bar{x}$.

tion generator (NF Corporation: WF1947) and a high-speed bipolar amplifier (NF Corporation: HSA4101) during the OFET operation. The light source for the TRM-SHG measurement was an optical parametric oscillator (OPO) (OPO: Continuum Surelite OPO, optical power: <300 μJ, and repetition rate:10 Hz). Fundamental light (wavelength was 1120 nm) was focused onto the channel region of the OFET with normal incidence using a super long working distance (WD) objective lens (Mitutoyo: M Plan Apo SL20×, NA=0.28, and WD=30.5 mm). Spot size was approximately 150 μm, and fundamental light almost uniformly irradiated across the channel. Spatial and temporal resolutions were 1 μm and 20 ns, respectively. Finally, second-harmonic (SH) light was detected by a cooled CCD camera (Andor Technology: DU420-BV). For the time-resolved measurement, timing between the voltage pulse applied to the OFET and laser pulse was precisely controlled.

To better understand the TRM-SHG experiment, we simulated the transient distribution of the carriers and electric field in an injection-type pentacene OFET. Figure 1(b) shows the top-contact structure of the OFET and the simulation parameters. Because the channel width in the experiment is far larger than its thickness and length, we are only interested in the carrier dynamics on the 2D cross section of the OFETs. Significant influence owing to the difference in the geometrical sizes between the simulation and experiment can be discarded because the magnitude of the electric field E_x in the simulated device is comparable with that in the actual experimental size about 1.0 and 2.3 V/μm along the channel direction (x direction) of the OFET in the simulation and experiment, respectively. The mobility was assumed to be 0.01 $cm^2/(V\ s)$ and independent of electric field. The relative dielectric constant of the pentacene was three.[11] Only the hole carriers were presented in the simulation because the pentacene OFET works as a p-type device, which was also confirmed by previous experimental observation.[10] The simulation was carried out by self-consistently solving 2D coupled diffusion drift and Poisson equations.[12] We modeled the contacts as thermionic emission controlled[13,14] with an injection barrier of 0.2 eV, and the holes could not penetrate through the boundary between the pentacene layer and insulator.

Figure 2(a) shows a typical TRM-SHG imaging at a delay time of 100 ns under $V_{gs}=-100$ V. With an increasing delay time, the SHG peak moves from the source to the drain electrode. Figure 2(b) shows the peak position of the SHG intensity vs the measured time in $\log_{10}$-$\log_{10}$ scale. The peak position was defined as a distance between the source electrode edge and the SHG peak. Five different gate-source voltages V_{gs} were applied in the experiment. The most outstanding feature is that for the each applied voltage the logarithm of the peak position $\bar{x}$ linearly depends on the logarithm of time t. Fitting showed that a simple relationship, $\bar{x}=\alpha t^{\gamma}$ with $\gamma \approx 1/2$ well describes the data. In the following, we call this relationship diffusionlike due to its similarity with the definition of diffusion.[15] The fittings also implied α to be a function of V_{gs}. Intriguingly, the diffusionlike behavior was also observed even when the TRM-SHG experiment was conducted at low and high temperatures (268–343 K, data not shown).

It should be interesting to see whether the simulation also yielded the same result. Figure 3 shows the carrier density and potential profile as functions of time and position x at the interface between the pentacene and insulator[16] after switching the gate and drain voltages to −5 V at $t=0$. Several interesting features were revealed. First, the carrier density

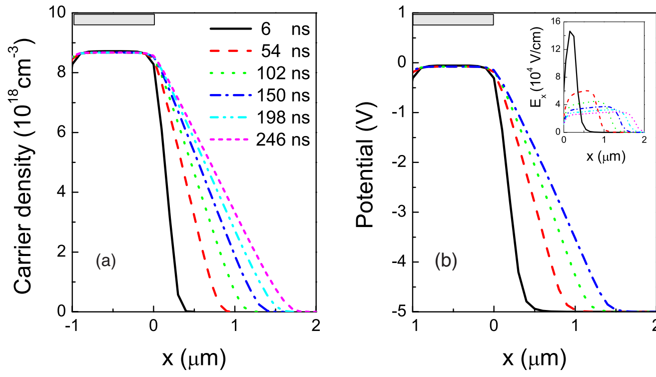

FIG. 3. (Color online) The simulated transient profiles of (a) the carrier density and (b) potential along the channel at the insulator and film interface. The applied V_{gs} is −5 V. The inset in panel (b) shows the electric field E_x. The gray bars at the top of the two panels represent the regions of the source electrodes.

and potential under the source are almost invariable after a very short time (<1 ns). Particularly, the potential is very close to the source voltage (0 V here) with a negligible drop. The negligible potential drop suggests that the carriers are sufficiently supplied into the pentacene from the source, and the carrier motion is limited by a transport process under these simulation parameters, which is similar to the space-charge limited current mechanism in a steady state.[5] Second, the profiles of the density and potential after 50 ns seem linearlike except for their leading edges. Finally, the inset in Fig. 3(b) shows that the peak position of E_x indeed migrates along the channel. Moreover, the peak position is very close to the forefront in the linear part of the carrier density, which supports our aim of probing carrier dynamics in materials using the TRM-SHG technique. To see whether the migration of the peak of the electric field also follows the diffusionlike behavior, we plotted the peak position vs time in $\log_{10}$-$\log_{10}$ scale in Fig. 4(a). The other simulated data at the gate and drain voltages of −8 and −2 V were also included there [Fig. 4(a)]. We met the diffusionlike migrations again.

These above features revealed by the simulation could be understood qualitatively. After nonzero gate and drain voltages are applied to the OFET, a large amount of holes is injected from the source electrode and rapidly accumulates at the interface between the pentacene and insulator under the source. These accumulated positive charges then build a local potential and the potential approaches the value of the source voltage immediately. Because of the drop along the channel direction between the new built potential and the gate voltage, an electric field E_x is yielded simultaneously and transports the holes along the channel. Notably, E_x does not result in a decay of the carrier density under the edge of the source with time because if the density there decays, it will induce a strong injection current from the edge of the source to compensate the loss of the carriers.[17] Apparently, these drifted holes can also raise the local potential, which decreases the potential drop and results in the decay of the field E_x, as shown in the inset of Fig. 3. Therefore, it might be expected that the expansion of the holes at the interface between the pentacene and insulator is $\propto t^{\gamma}$ with $\gamma<1$.

In order to determine the factor γ, we presented a quantitative analysis that is mainly inspired by the simulation. Because the carrier dynamics determine the transient electric field in the OFET, we first approximate the carrier density $p(x,t)$ at the interface between the pentacene and insulator as

$$p(x,t) \simeq h[1 - x/(\alpha t^{\gamma})], \tag{1}$$

where h is the time-invariable carrier density under the source, αt^{γ} with constants α, and γ represents a distance that is an extrapolation of the linear part of the carrier density and where the density becomes zero. We see from Fig. 3 that this distance slightly underestimates the region of the nonzero carrier density. The reason for proposing this "phenomenological" formula could be easily understood from Fig. 3(a). Equation (1) is valid only for x between zero and αt^{γ} and the time after the establishment of a linear density. Substituting Eq. (1) into the drift-diffusion equation for hole at the interface, $\partial_t p(x,t) = -\partial_x[p(x,t)\mu E_x(x)] + D\partial_x^2 p(x,t)$ with the hole mobility μ and diffusion coefficient D, we have

$$\frac{\gamma h x}{\alpha t^{\gamma+1}} \simeq -\partial_x[\mu E_x(x)]p(x,t) + \mu E_x(x)\frac{h}{\alpha t^{\gamma}}. \tag{2}$$

Here we neglected the current component vertical to the interface in that the carriers could not pass through the interface. Let $\bar{x}$ be the peak position of the electric field, i.e., $\partial_x E_x(\bar{x})=0$. Then if $\bar{x} \leq \alpha t^{\gamma}$, the first term in the right-hand side of Eq. (2) vanishes at $\bar{x}$. We further approximate $E_x(\bar{x}) \simeq -V_{gs}/\bar{x}$. This approximation should be good because the potential along the channel is linearlike; see the inset in Fig. 3(b).[18] Thus, we obtain the following relation:

$$\mu \simeq \frac{\gamma}{|V_{gs}|}\frac{\bar{x}^2}{t}. \tag{3}$$

Remarkably, because the simulation showed that the peak position of the electric field is very close to the forefront of the linear part of the carriers, we expect that γ equals 1/2 approximately. Note that the above derivation also holds for a field-dependent mobility because if the mobility is a function of the electric field, $\mu[E_x]$, the first term in the right-

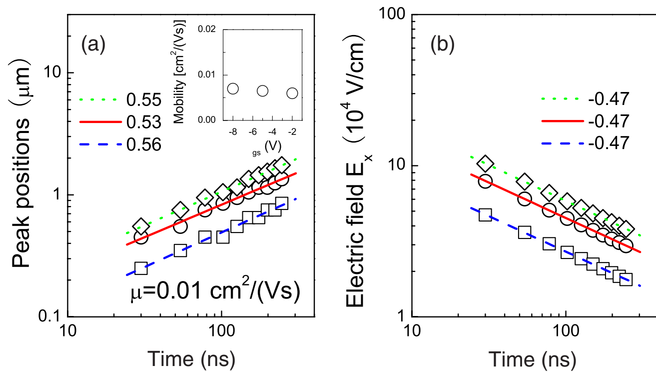

FIG. 4. (Color online) The simulated position (a) and value (b) of the peak of the electric field vs time. The applied V_{gs} are −2 V (squares), −5 V (circles), and −8 V (diamonds), respectively. The lines are the corresponding fittings and their slopes were listed. The inset in (a) are the mobilities evaluated by Eq. (3) with $\gamma=1/2$ at the three V_{gs}.

hand side of Eq. (2) becomes $\partial_x\{\mu[E_x]E_x\}(x) = \partial_x E_x(x)\{\mu[E_x](x) + E_x(x)\partial_{E_x}\mu[E_x](x)\}$, which still vanishes at the position $\bar{x}$. On the other hand, Eq. (3) could be derived by a simpler dimensionality argument. First we may define a velocity $v = \bar{x}/t$. Due to $v \propto \mu E_x(\bar{x})$ and the approximation of $E_x(\bar{x})$ above, we immediately obtain $\mu \propto \bar{x}^2/(|V_{gs}|t)$. However, this derivation neither tells us the numerical coefficient nor has physical justification.

Equation (3) includes several important predictions. First of all, the peak position of the electric field (or SHG intensity in the experiment) migrates in terms of the square root of time.[19] Both the experiment and simulation have confirmed this prediction. Second, the square-root dependence of Eq. (3) does not matter with the real power exponent of γ. This relation would be universal in the TRM-SHG experiment. Finally, Eq. (3) also reminds us that $E_x(\bar{x}) \approx \sqrt{|V_{gs}|/t\mu} \propto t^{-1/2}$. Although the experiment did not provide such type of data, we readily test this relationship by a comparison with the simulated data; see Fig. 4(b). The agreement between the prediction and data is good.

The relationship in Eq. (3) provides us a method to evaluate the mobility from the SHG experimental data. We first evaluated the mobility from the simulation data with $\gamma = 1/2$ to test its precision; see the inset in Fig. 4(a). A slightly larger $\gamma \sim 0.7$ may give a better estimation. We also applied Eq. (3) to the real experimental data in Fig. 2(b) and showed the mobilities in Fig. 2(c); $\gamma = 0.7$ was chosen there. To take into account the possible dependence of the mobility on the electric field, we listed them with respect to the electric field E_x calculated by $-V_{gs}/\bar{x}$ at each peak position. We see that the mobility weakly depends on the electric field if any, while the dependence on the gate voltage seems doubtless.[20,21]

In this work we applied the TRM-SHG technique to study the migration of the peak of the electric field along the OFET channel. Under a broad range of experimental conditions, this migration always follows a diffusionlike behavior. Our numerical simulation and general physical argument further confirmed this observation. The good agreement between the data and the simple theory is very intriguing because the mechanism of carrier transport in organic materials, such as the pentacene here, could be considerably complicated at microscopic levels.[7–9] Because the current work focused on the movement of the peak position of the SHG intensity, other experimental information, e.g., the intensity and the decay form of the SHG signal, was still not investigated systematically. Our next task would explore the TRM-SHG technique to identify more characteristics of organic conductive materials from the transient profiles of the SHG intensity.

T.M. thanks the New Energy and Industrial Technology Development Organization (NEDO) for financial support. F.L. would like to thank Tokyo Institute of Technology for their hospitality, where this work was completed. The Grants-in-Aid for Scientific Research (Grants No. 18686029 and No. 19206034) are also gratefully acknowledged.

---

*manaka@ome.pe.titech.ac.jp
†iwamoto@pe.titech.ac.jp
[1] G. M. Sessler, *Electrets* (Springer, Berlin, 1980).
[2] H. Meier, *Organic Semiconductors: Dark and Photoconductivity of Organic Solids* (Chemie, Weinheim, 1974).
[3] J. R. Haynes and W. Shockley, Phys. Rev. **81**, 835 (1951).
[4] R. G. Kepler, Phys. Rev. **119**, 1226 (1960).
[5] P. Laurenceau, G. Dreyfus, and J. Lewiner, Phys. Rev. Lett. **38**, 46 (1977); G. M. Sessler, J. E. West, and R. Gerhard, *ibid.* **48**, 563 (1982).
[6] M. Iwamoto, Y. Majima, H. Naruse, T. Noguchi, and H. Fuwa, Nature (London) **353**, 645 (1991).
[7] H. Scher and E. W. Montroll, Phys. Rev. B **12**, 2455 (1975).
[8] H. Bassler, Phys. Status Solidi B **175**, 15 (1993).
[9] P. M. Borsemberger, E. H. Magin, M. van der Auweraer, and F. C. De Schryver, Phys. Status Solidi A **140**, 9 (1993).
[10] T. Manaka, E. Lim, R. Tamura, and M. Iwamoto, Nat. Photonics **1**, 581 (2007).
[11] Y. S. Lee, J. H. Park, and J. S. Choi, Opt. Mater. (Amsterdam, Neth.) **21**, 433 (2002).
[12] C. M. Snowden, *Semiconductor Device Modelling* (Peter Peregrinus, London, 1988).
[13] P. S. Davids, I. H. Campbell, and D. L. Smith, J. Appl. Phys. **82**, 6319 (1997).
[14] N. Tessler and Y. Roichman, Appl. Phys. Lett. **79**, 2987 (2001).
[15] C. W. Gardiner, *Handbook of Stochastic Methods: For Physics, Chemistry and the Natural Sciences* (Springer, Berlin, 1983).
[16] Because the carriers are mainly confined at the interface between the pentacene and insulator, and the electric-field profile E_x is almost invariable along the depth of the OFET, we only focused on the carrier density and electric field at the interface in this work.
[17] If the source could not provide enough injection carriers to compensate the loss of the carriers under the edge of the source, the migration of E_x would be completely different from what we discussed here. We have observed this phenomenon in the TRM-SHG experiment.
[18] The approximation of the electric field is crucial to the accuracy of Eq. (3). The simulation showed that it would be good at a relatively large time after a switching of the gate and drain voltages.
[19] In our previous paper (Ref. 10), the carrier motion was analyzed in accordance with standard time-of-flight approach, where linear carrier motion with time was assumed.
[20] G. Horowitz, R. Hajlaoui, and P. Delannoy, J. Phys. III **5**, 355 (1995).
[21] A. R. Brown, C. P. Jarrett, D. M. de Leeuw, and M. Matters, Synth. Met. **88**, 37 (1997).